

Multilayered double perovskite Ferroelectric for Green High-Performance Self-Powered X-ray Detection

Zhangtong Han,^{[a], [b]} Qianwen Guan,^{[a], [b]} Huang Ye,^{*[a]} Yi Liu,^{[a], [b]} Jianbo Wu,^[a] Lijun Xu,^{[a], [b]} Chengshu Zhang,^[a] Hang Li,^{[a], [b]} Qiuxiao Yin^[a] and Junhua Luo^{*[a], [b]}

^a State Key Laboratory of Structure Chemistry, Fujian Institute of Research on the Structure of Matter, Chinese Academy of Sciences, Fuzhou, Fujian, 350002, P. R. China. Email: yehuang@fjirsm.ac.cn; jhluo@fjirsm.ac.cn

^b University of Chinese Academy of Sciences, Beijing, 100049, China.

Experimental Procedures

Materials: Cyclohexylmethanamine (97%, Adamas), Silver oxide (Ag_2O , 99.7%, Adamas), Bismuth carbonate (Bi_2CO_3 , 99.9%, Aladdin), cesium carbonate (99.5%, Aladdin), hydrobromic acid (HBr , 40%, Aladdin) were commercially purchased and used without further purification.

Synthesis and crystal growth: Compound $\text{CHMA}_2\text{CsAgBiBr}_7$ (**CCAB**) was prepared by mixing a stoichiometric ratio of cyclohexylmethanamine, caesium carbonate, Ag_2O and Bi_2O_3 the solution of concentrated hydrobromic acid. The saturated solution was heated and stirred at 373 K for 20 min to obtain the clarified solution. Single crystals of $\text{CHMA}_2\text{CsAgBiBr}_7$ were grown from saturated solution at 1 K/day by temperature cooling method.

Single crystal and powder X-ray diffraction: The PXRD patterns of powder were obtained by the MiniFlex 600, Rigaku at room temperature using a $\text{Cu K}\alpha$ rotating anode with an angular range of $5^\circ - 40^\circ$ in 0.02° steps. The XRD pattern and rocking curves for **1** bulk crystal were collected on a Rigaku SmartLab X-ray diffractometer.

The optical and photoelectric measurements: The diffuse reflection spectra of **CCAB** were performed on a PerkinElmer Lambda 950 UV-vis-NIR spectrometer. The current-voltage curve measurement was measured on a high-precision electrometer (Keithley 6517B).

Morphology Characterization: The surface morphology of the single crystals was acquired by scanning electron microscopy (SEM) and atomic force microscope (AFM) on a JEOL JSM6700-F field emission scanning electron microscope and Bruker Dimension ICON atomic force microscope, respectively.

Ferroelectric measurements: The P-E hysteresis loops were carried out on a ferroelectric analyzer (Radiant Precision Premier II) by the classical Sawyer-Tower circuit method. Two pairs of electrodes were formed orthogonally on a single crystal of **CABB** with silver paste. In order to avoid electric discharge at high electric field, single crystal of **1** was immersed in silicone oil to measure the P-E hysteresis loops.

X-ray detection: The current-voltage ($I-V$) traces and current-time ($I-t$) curves were recorded by using a Keithley 6517B high-precision electrometer under X-ray irradiation. A silver target (maximum power 4 W) X-ray tube with a maximum photon energy is 50 keV and a peak intensity is at 22 keV was used as the X-ray source (Mini-X2, Amptek, USA). The dose rate of the X-ray tube can be adjusted by changing its tube current measured by an X-ray dosimeter (Accu-Gold, Radcal, USA) attached to the $10\times 6-180$ ion chamber in an integrating mode.

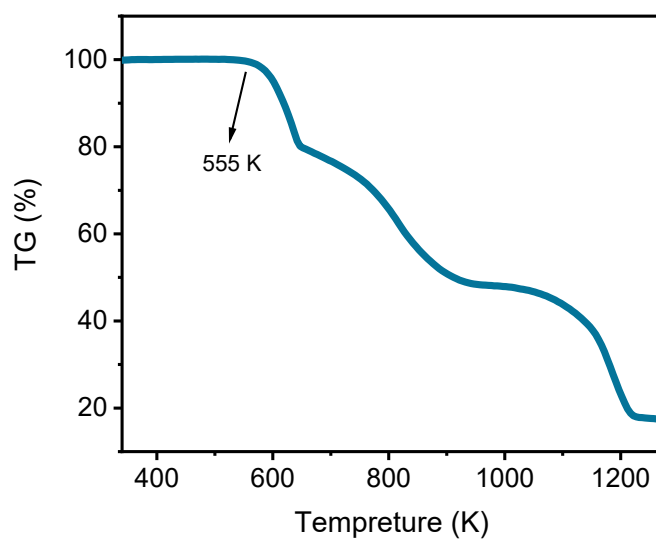


Figure S1. Thermal analysis of CCAB.

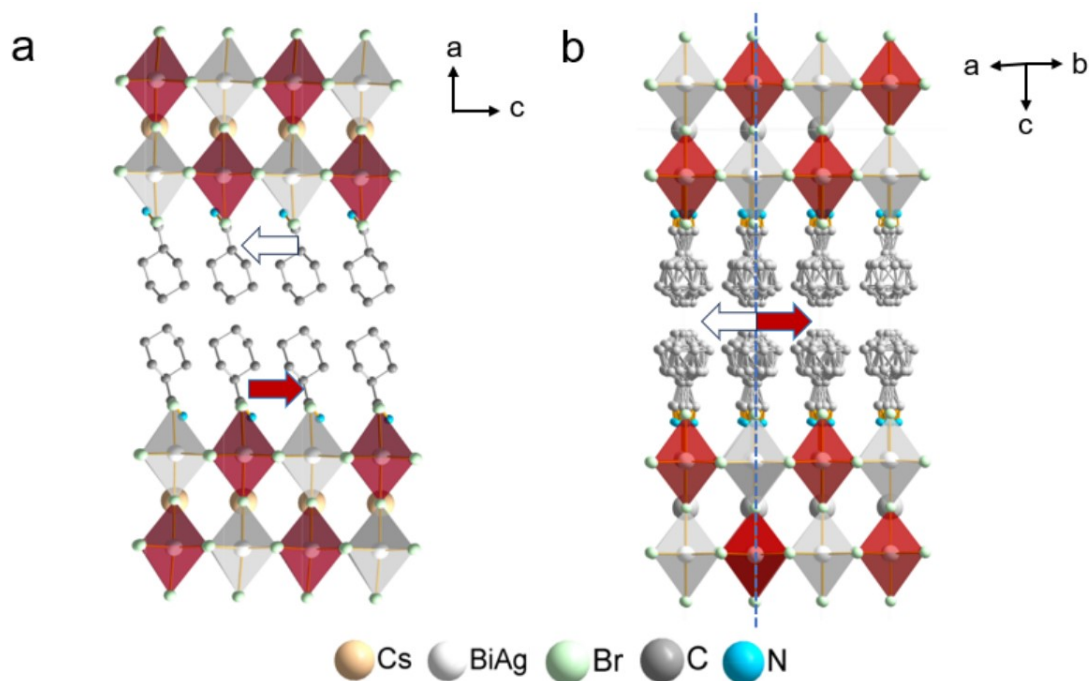


Figure S2. Crystal structures of CCAB. Diagram of crystal structure packings in the a AFEP at 360 K and b paraelectric HTP at 390 K. The white color shows the atomic co-occupancy of Ag and Bi.

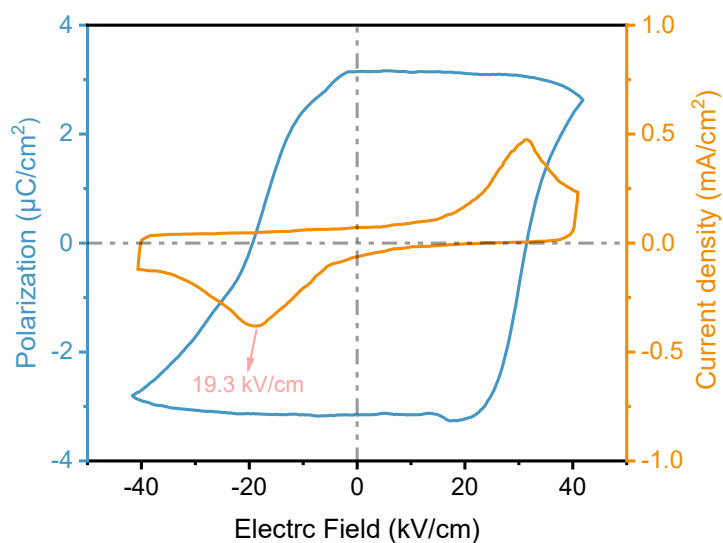


Figure S3. Ferroelectric hysteresis loop of **CCAB** along the *c* axes.

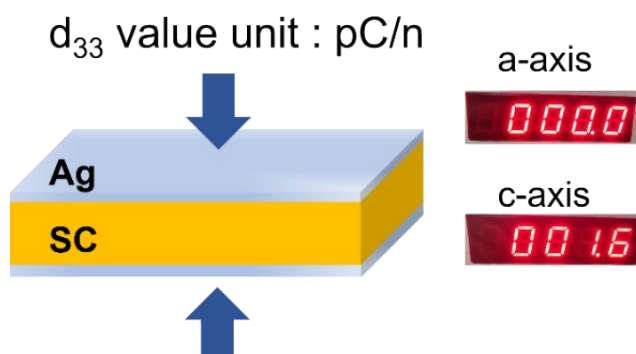


Figure S4. The piezoelectric schematic diagram and related d_{33} value along the *a* and *c* axes, respectively.

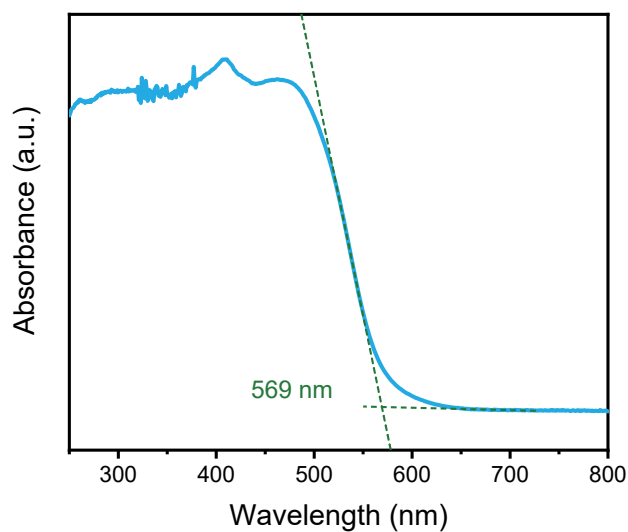


Figure S5. Absorption spectra of **CCAB**

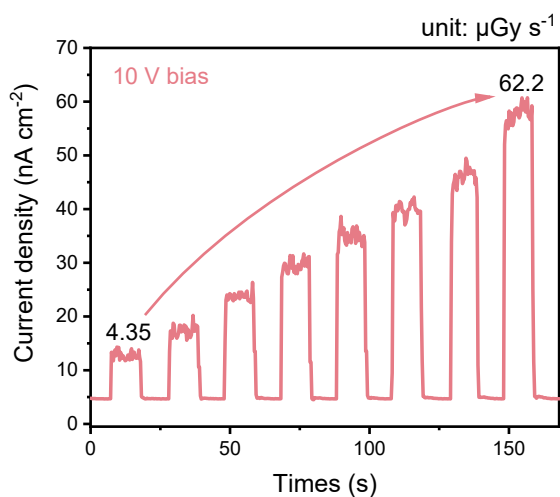
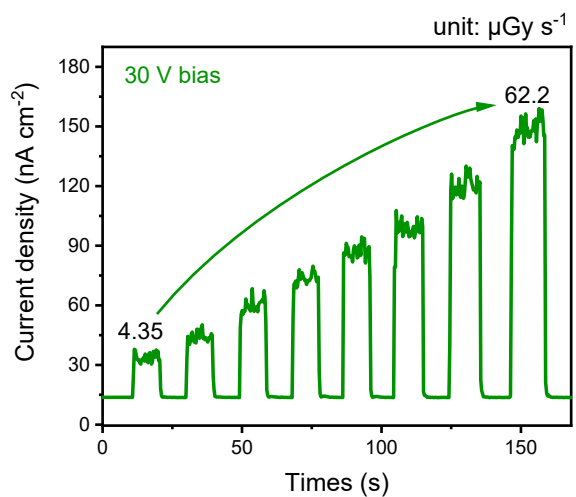


Figure S6. Current density-time curves of **CCAB** SC detector under 10 V bias.



SUPPORTING INFORMATION

Figure S7. Current density-time curves of **CCAB** SC detector under 30 V bias.

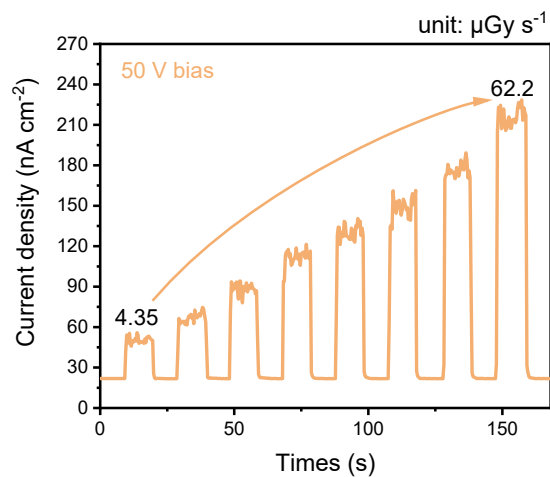


Figure S8. Current density-time curves of **CCAB** SC detector under 50 V bias.

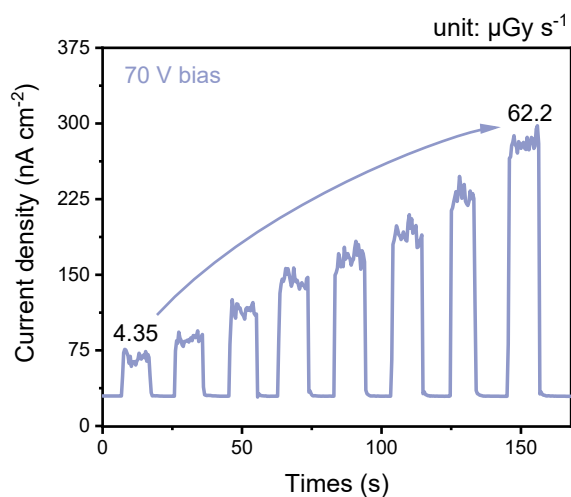
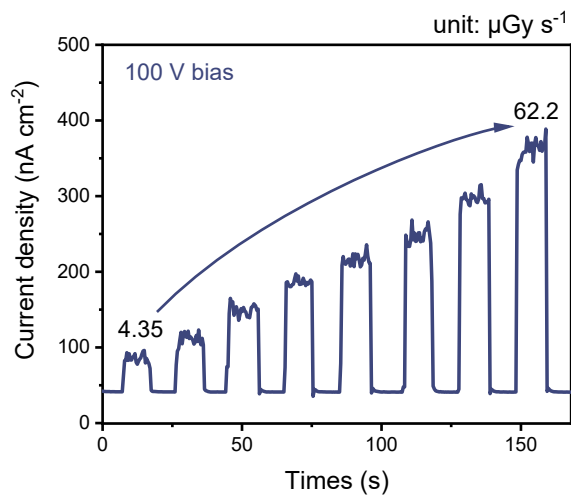


Figure S9. Current density-time curves of **CCAB** SC detector 770 V bias.



SUPPORTING INFORMATION

Figure S10. Current density-time curves of **CCAB** SC detector 100 V bias.

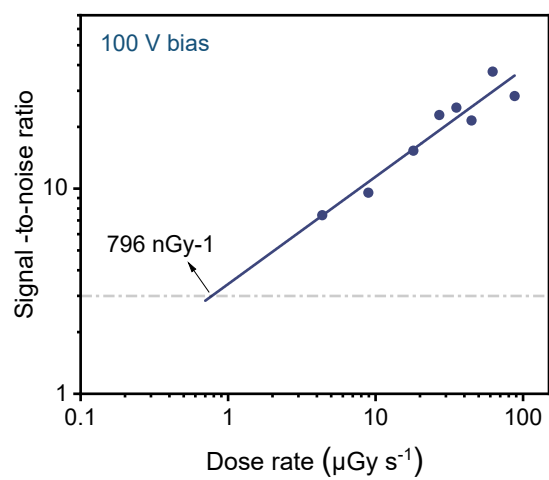


Figure S11. The detection limit of **CCAB** under 100 V biases